Development of an innovative energy management system for a railway smart grid

Aimad Chegra, Fawzia Amokrane, Nada Zouzou, Smail Ziani, Tony Letrouve, Hervé Caron

Development of an innovative energy management system for a railway smart grid

Chegra Aimad
IRT Railenium
Valenciennes, France
aimad.chegra@railenium.eu

Amokrane Fawzia
IRT Railenium
Valenciennes, France
fawzia.amokrane@railenium.eu

Zouzou Nada
IRT Railenium
Valenciennes, France
nada.zouzou@railenium.eu

Ziani Smail
IRT Railenium
Valenciennes, France
smail.ziani@railenium.eu

Letrouve Tony
SNCF RESEAU
Paris, France
tony.letrouve@reseau.sncf.fr

Caron Herve
SNCF RESEAU
Paris, France
herve.caron@reseau.sncf.fr

***Abstract*—The anticipated growth in railway traffic in the coming years primarily affects the 350 Direct Current substations in France, which suffer from a relatively low voltage level of 1500V. This situation limits the power of the locomotives and prompts stakeholders in the electrification system to seek innovative solutions to ensure the necessary energy supply. One of the solutions considered is the integration of solar energy production systems and storage systems within the fixed electric traction installations. In this context, a novel collaborative project with a group of industrial and academic partners called RACCORD proposes an innovative solution by suggesting the integration of solar energy production and energy storage systems within the fixed electric traction installations. This approach aims to strengthen the network, increase the voltage in the catenary, reduce the carbon footprint, and improve the efficiency and capacity of transport networks. This paper develops a model and an innovative method for energy management of this railway smart grid. Finally, a simulation analysis was conducted to evaluate the operation of this railway smart grid.**

***Index Terms*—Railway smart grid, Energy management system, Modelling**

I. Introduction

Since the beginning of the 20th century, various Direct Current (DC) and Alternating Current (AC) rail electrification systems have been developed in Europe. There are 15,000 km of electrified lines on the French National Railway Network (FNRN), with 60% of these lines electrified by 25 kV/50 Hz AC and 40% by 1.5 kV DC. The DC rail network currently suffers from relatively low voltage levels, which limit the power of the locomotives that can use these lines and the density of traffic due to the high currents in the catenary. The catenary's copper cross-sections are very large, up to 1000 mm² in some high-traffic areas. In this context, the French National Railway Company (SNCF) is working to improve its energy performance by 20% by 2025 compared to 2015. SNCF has formed a consortium to bring together the best of the French rail industry around a shared goal to reinforce the rail power supply network by integrating renewable energy sources and energy storage elements. The innovative proposed project is named RACCORD. The consortium is composed of different partners, including Railenium, with complementary roles. The RACCORD project proposes an innovative solution by integrating solar energy production systems (photovoltaic panels (PV) with a peak power of around 500 kW and a surface area of 2000 m²) and 1800 kWh energy storage systems (ESS) within the fixed electric traction installations. This approach aims to strengthen the network, increase the voltage in the catenary, reduce the carbon footprint, and improve the efficiency and capacity of transport networks. By 2026, a test site will allow for the experimentation and validation of the technological components implemented, and for the integration of renewable energy sources on SNCF Réseau's property. Before proceeding to experimental implementation, it is necessary to simulate different architectures and use cases for this railway smart grid. A robust method is needed to manage the energy flows of the system, respecting the physical constraints of each component of this railway smart grid. An innovative method for the energy management system (EMS) is proposed to split the power between the railway substation, ESS, and PV. Several EMS methods can be implemented for this case: optimized-based methods, such as Linear Programming [1], Sequential Quadratic Programming (SQP) [2], Dynamic Programming (DP) [3], Particle Swarm Optimization [4], Genetic Algorithm (GA) [5], etc.; rule-based methods, such as fuzzy logic [6] and deterministic rules-based [7]; and machine learning-based methods, such as reinforcement learning [8] and multi-agent systems [9].

This paper develops an innovative method for energy management of this railway smart grid. The first part involves comprehensive modelling, including three direct current DC substations, as well as an electricity production system through photovoltaic panels, complemented by an energy storage system in the form of batteries. It also addresses the sizing of an MPPT converter for the PV system and a bidirectional

979-8-3503-7390-5/24/$31.00 © 2024 European Union

converter for the storage system. The second part consists of the development of a two-stage energy management system, which includes day-ahead energy management (DAEM) and real-time energy management (RTEM). DAEM aims to minimize the energy drawn from the grid based on forecasted data, while RTEM aims to adjust the battery power based on real-time measurements of consumption and production from the PV system. Finally, a simulation analysis was performed to validate the operation of this railway smart grid.

The rest of this paper is organized as follows. Section II details the model of the proposed railway smart grid. Section III introduces the energy management strategy that is used. Section IV presents the simulation results, followed by the conclusion in Section V and perspectives in Section VI.

II. Modeling of the RACCORD System

This section details the model for the new railway smart grid (RACCORD system) shown in Figure 1. The system model comprises three DC substation models (the substation where the demonstrator will be installed and the two adjacent substations), the ESS model, and the PV model with DC/DC converters connected to their outputs.

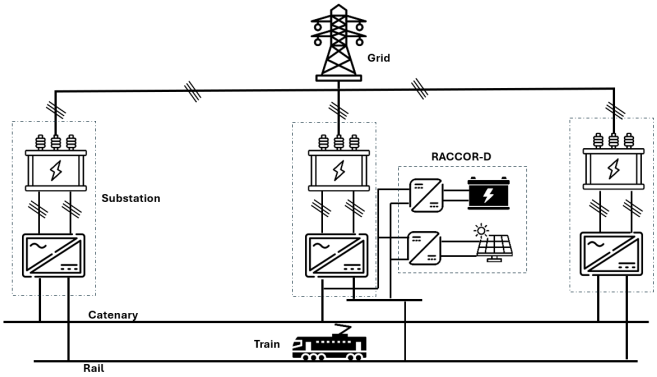

Fig. 1: Global schematic of the new railway smart grid.

A. Modeling of the Three DC Substations

In practice, in the DC case, the current that powers a train does not come from a single substation, but from several substations located along its line. The contribution of each substation varies based on its distance from the train. However, the majority of the power comes from the two substations on either side of the train when it is positioned in the middle of their locations. For a more realistic simulation, it is judicious to model three DC substations.

The DC railway substation consists mainly of a transformer-rectifier unit. The transformer used is a step-down three-phase transformer whose input is connected in star and linked to a 64 kV voltage network. It has two outputs: the first is connected in star and the second is connected in delta, both with a voltage of 1430 V. This specific coupling generates a 30° phase shift between the two outputs, which is important for the proper functioning of the electrical system. The phase shift helps in reducing harmonic distortions and for the synchronization of the equipment connected to the substation. This type of transformer is commonly used in railway substations to lower the voltage from the high-voltage network to a voltage suitable for powering rolling stock and railway infrastructure.

Two three-phase double-alternate rectifiers are used, each connected to one output of the transformer. Their outputs are then connected in parallel. This configuration offers several significant advantages. Firstly, having two rectifiers in parallel distributes the load between them, reducing the current intensity on each rectifier. This helps to balance the load better and reduce the risk of overload. Additionally, the two inputs of the rectifiers are phased by 30°, creating a direct voltage with 12 pulses.

The advantage of this setup is that it reduces ripples in the direct voltage produced by the rectifiers. The additional pulses help improve the quality of the direct voltage, making it more stable and consistent [11].

B. Battery Modelling

For the RACCORD project, batteries using lithium iron phosphate technology (LiFePO4 or LFP) have been selected. In this paper, the model used for the battery is a linear simple model [10]. It consists of a controllable voltage source with a mean voltage V_{oc} and an internal resistance which models the energy losses. The battery terminal voltage V_{bat} is calculated applying Kirchhoff's law, assuming the battery current I_{bat} is positive during discharging operation. However, when a load is connected, this voltage is given by:

$$V_{bat} = V_{oc} - R_{int} I_{bat} \tag{1}$$

V_{oc}, the battery open circuit voltage, and internal resistance R_{int} depend on the battery state of charge (SoC). The battery charge increases if the current is negative (charging operation) or decreases if it is positive (discharging operation):

$$\dot{SoC}(t) = -\frac{I_{bat}(t)}{Q_{nom}} \tag{2}$$

Q_{nom} is the nominal battery capacity in Ah.

C. Modeling of the bidirectional DC/DC converter in current mode

The bidirectional DC/DC converter, or buck/boost converter, is essential in the energy management of storage systems, such as batteries. Its current switching functionality allows for precise regulation of the battery charging and discharging processes. Figure 2a illustrates the electrical circuit of a bidirectional DC/DC converter. In this context, K_1 and K_2 act as switching devices. The parameters $I_{L_{bat}}$ and $V_{L_{bat}}$ characterize the current and voltage across the inductor L, respectively. Similarly, I_c and V_c represent the current and voltage at the capacitor terminals. Finally, I_s denotes the output current of the converter.

The operation of the converter is segmented into two distinct phases:

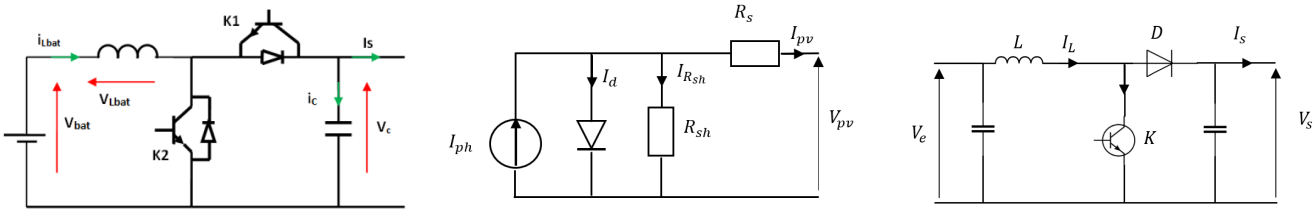

(a) Electrical diagram of the bidirectional DC/DC converter.

(b) Electrical diagram of the photovoltaic panel.

(c) Electrical diagram of the boost converter.

Fig. 2: Electrical diagrams of RACCORD system components

1) Boost Phase: The chopper operates in Boost mode, activating the IGBT of switch K_2 and the diode of switch K_1. The electrical relations are expressed by:

$$\begin{cases} V_{L_{bat}} = V_{bat} - (1-\alpha)V_c \\ I_c = (1-\alpha)I_{L_{bat}} - I_s \end{cases} \quad (3)$$

2) Buck Phase: The chopper operates in Buck mode, involving the IGBT of switch K_1 and the diode of switch K_2. The operating equations are:

$$\begin{cases} V_{L_{bat}} = (1-\alpha)V_c - V_{bat} \\ I_c = I_s - (1-\alpha)I_{L_{bat}} \end{cases} \quad (4)$$

By exploiting equations 3 and 4, the average model of the operation of the buck/boost chopper in reversible mode can be established as follows:

$$\mp \begin{cases} V_{L_{bat}} = (1-\alpha)V_c - V_{bat} \\ I_c = I_s - (1-\alpha)I_{L_{bat}} \end{cases} \quad (5)$$

D. Regulation of the bidirectional Buck/Boost converter

The main objective of the converter in this study is to regulate the output current $I_{L_{bat}}$ of the battery, which depends on the duty cycle α. The duty cycle defines the duration during which the switch remains active. Adjusting this ratio aligns the output current with the reference I_{ref}, thus ensuring precise management of the battery's charge or discharge state. The state model of the converter is expressed as follows:

$$\begin{bmatrix} \frac{dI_L}{dt} \\ \frac{dV_c}{dt} \end{bmatrix} = \begin{bmatrix} 0 & -\frac{(1-\alpha)}{L} \\ \frac{(1-\alpha)}{C} & -\frac{1}{RC} \end{bmatrix} \begin{bmatrix} I_L \\ V_c \end{bmatrix} + \begin{bmatrix} \frac{1}{L} \\ 0 \end{bmatrix} V_{bat} \quad (6)$$

Linearizing around the equilibrium point $I_L = I_{eL} + \tilde{I_L}$, $V_c = V_{ec} + \tilde{V_c}$, and $\alpha = \alpha_e + \tilde{\alpha}$. Where $\tilde{V_c}$, $\tilde{I_L}$, and $\tilde{\alpha}$ represent small variations, for more details see [12]. The transfer function relating the inductive current to the duty cycle is determined by:

$$H(p) = \frac{\tilde{I_L}}{\tilde{\alpha}} = \frac{2 \cdot V_{ec}}{R(1-\alpha_e)^2} \frac{1 + \frac{R \cdot C}{2}p}{\frac{L \cdot C \cdot p^2}{(1-\alpha_e)^2} + \frac{L \cdot p}{R \cdot (1-\alpha_e)^2} + 1} \quad (7)$$

To regulate the battery output current, a proportional-integral (PI) controller is implemented. Its transfer function is expressed as follows:

$$C(p) = K_p + K_i/p \quad (8)$$

where K_p and K_i are the controller coefficients, determined using the *PID Tuner* tool in MATLAB.

E. Modeling of the Photovoltaic system

Solar energy, a renewable resource, is gradually becoming an essential component of global energy production. Photovoltaic panels transform solar energy into electricity through the photovoltaic effect. The electrical representation of a photovoltaic panel is shown in Figure 2b. The current produced by the photovoltaic cell, I_{pv}, is described by:

$$I_{pv} = I_{ph} - I_0 \left(e^{\left(\frac{q(V_{pv} + R_s I_{pv})}{aKT}\right)} - 1 \right) - \frac{V_{pv} + R_s I_{pv}}{R_{sh}} \quad (9)$$

where I_{ph} is the photocurrent, and I_0 is the diode saturation current. The terms q, a, k, and T represent the electron charge, the diode ideality factor, the Boltzmann constant, and the cell temperature in Kelvin, respectively. V_{pv} is the voltage across the photovoltaic cell, and R_s and R_{sh} are the series and parallel resistances of the cell.

The photocurrent I_{ph} is a function of the solar irradiance G and the cell temperature, as described by:

$$I_{ph} = I_{sc} + k_i(T - 298.15) + G/1000 \quad (10)$$

Here, I_{sc} is the short-circuit current, k_i is the temperature coefficient of the short-circuit current, and G is the solar irradiance in watts per square meter. Thus, equations 9 and 10 demonstrate the sensitivity of the current generated by the photovoltaic cell to variations in solar irradiance G and temperature T.

The reverse saturation current of the diode, denoted I_0, is defined by the following equation:

$$I_0 = \frac{I_{sc} + k_i(T - T_{ref})}{e^{\frac{q\left(V_{oc} + K_v\left(T - T_{ref}\right)\right)}{aKT}} - 1} \quad (11)$$

In the presented equation, I_0 represents the diode saturation current, which denotes the maximum current that can flow through the diode under reverse bias condition for a specific applied voltage. On the other hand, V_{oc} expresses the open-circuit voltage of the photovoltaic cell, i.e., the maximum voltage obtained in the absence of an external load. The coefficient K_v quantifies the variation of the open-circuit voltage V_{oc} with temperature, thus indicating the thermal sensitivity of the photovoltaic cell voltage.

F. Modeling of a Boost Converter

The boost converter increases the output voltage by alternating the operation of its components: an inductor (L) and two switches (K and D). By closing switch K, energy is stored in the inductor. When K opens and D closes, this energy is released to the load, increasing the output voltage. This process is regulated by the duty cycle of the switches, which controls the magnitude of the voltage boost. The relationship between the output voltage and the duty cycle in a boost converter is given by the following equation [13]:

$$V_s = V_e/(1-\alpha), \tag{12}$$

where V_s represents the output voltage, V_e is the input voltage, and α symbolizes the duty cycle.

G. Maximum Power Point Tracking (MPPT) Control

The MPPT control is a technique used in photovoltaic systems to optimize the conversion of solar energy into electricity. The MPPT control continuously adjusts the voltage and current to keep the solar panels at the maximum power point, adapting to changes in brightness or temperature, thereby improving the efficiency and profitability of the installations. In contrast, the Perturb and Observe (P&O) control periodically modifies the current or voltage and observes the impact on the power produced to find this optimal point. It adjusts the direction of the perturbation based on the observed results to maximize energy production [14].

III. Energy Management

The electrical railway system is consistently one of the largest energy consumers. With the significant rise in electricity consumption from distributed resources in French railways, adapting energy management strategies to optimize costs is crucial. In this paper, the goal of railway energy management is to optimize the energy costs required for the operation of the rail system by privileging PV production and storing energy during off-peak hours when prices are lower, to utilize it during peak hours when prices increase. To ensure optimal performance, a two-tier energy management approach is implemented:

A. Day-ahead Energy Management (DAEM)

Day-ahead energy management (DAEM) is a strategy that anticipates energy requirements for the following day based on predictions of PV production and substation consumption. It helps to optimize the allocation of energy resources by predicting when to store energy or when to consume it directly according to needs. It also considers constraints affecting each system. In this paper, an optimization-based energy management system is used.

1) Objective Function: The objective function that we wish to minimize over each prediction horizon H_p corresponds to the cost of energy, i.e., the cumulative sum of the product of the electricity purchase rate C_{RTE} according to the TURPE 6 [15] pricing grid and the power drawn from the substation P_{sst} over a time step T_e. The parameters of the optimization problem are the substation power vector P_{sst} and the power exchanged with the storage system P_{Bat}. The objective function is given by:

$$J = \min \left(\sum_{k=1}^{H_p} C_{RTE}(k)\, P_{sst}(k)\, \Delta t \right) \tag{13}$$

The prediction horizon H_p chosen for this study corresponds to a duration of 24 hours, with a time step T_e of 10 minutes, which matches the time step of the predicted data.

2) Constraints: The system constraints include limitations on the stored energy and battery power:

$$\begin{cases} E_{Bat_{min}} < E_{Bat} < E_{Bat_{max}} \\ P_{Bat_{min}} < P_{Bat} < P_{Bat_{max}} \end{cases} \tag{14}$$

To prevent the sending back of energy to the grid and also to not exceed the subscribed power, substation power limits are set:

$$P_{sst_{max}} > P_{sst} > P_{sst_{min}} \tag{15}$$

Finally, it is also necessary to consider constraints related to grid balance.

$$P_{Load} = P_{sst} + P_{PV} + P_{Bat} \tag{16}$$

3) Choice of Optimization Algorithm: To identify a minimum of the defined objective function, we opted for the sequential quadratic programming (SQP) algorithm, frequently used in energy management because of its ability to locate a global minimum while respecting the constraints imposed.

B. Real-Time Energy Management (RTEM)

Real-time energy management offers the possibility of fine-tuning the solution planned for the DAEM, taking into account prediction errors and power fluctuations. This means that decisions made for DAEM can be adjusted in real time to better suit observed reality. This flexibility is particularly important given that the data used for DAEM are generally averages over relatively long time intervals. By integrating this real-time energy management (RTEM), the system can react effectively to unexpected events using measurements of PV system output and substation consumption. In this paper, a rule-based EMS is used, as shown in Figure 3.

IV. Simulation Results

For this study, in the absence of predictive consumption data, we used actual measurements. For photovoltaic (PV) panel production data, we have a GHI forecast profile for the following day. For pricing, we used a variable profile extracted from TURPE 6. At the start of the simulation, the DAEM is executed. The results of this energy management will be automatically integrated into the simulation to initiate RTEM. The simulation period will be one day, with a time step of 1 millisecond. The energy management parameters are shown in Table I.

The simulation results are shown in Figures 5, 6, and 7.

Figure 4 shows the power associated with the consumption and production of photovoltaic (PV) panels. The orange curve

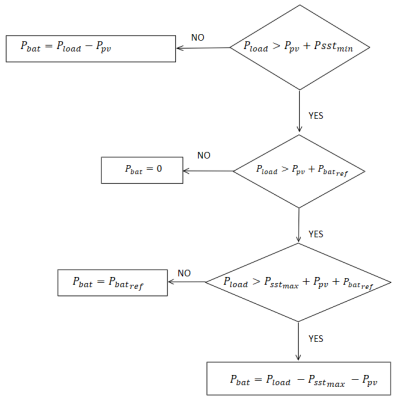

Fig. 3: Real-Time energy management method

TABLE I: Energy Management Parameters

Characteristics	Value
Peak Power of PV	500 kW
Max Power of Storage System	1.2 MW
Min Power of Storage System	−1.2 MW
Energy Capacity of Storage System	1.84 MWh
Subscribed Power	2 MW
Max Transformer Power	4 MW
Simulation duration	24 h
Step time	1 ms

shows the power consumed by the load measured every second, while the red curve represents the average consumption over ten-minute intervals. This average was calculated due to the absence of predicted data for 10 minutes. The light blue curve shows the actual irradiation captured by the PV panels, while the black blue curve shows the predicted irradiation withe step time of ten-minute. The light blue and red curves will be used for DAEM, while the orange and black blue curves will be used for RTEM.

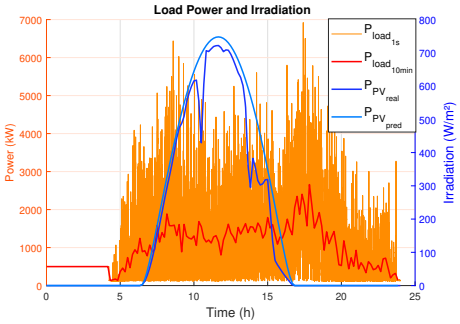

Fig. 4: Power Evolution and Irradiations

Figure 5 shows the power output of the substation. The blue curve corresponds to the data obtained with RTEM, while the red curve represents the data with DAEM. The yellow line indicates the subscribed power, and the purple line represents the maximum power the substation can support.

It is observed that the energy management largely respects the imposed constraints. The red power curve consistently stays below the yellow line, corresponding to the subscribed power. However, the blue curve occasionally exceeds the purple line, representing the maximum power, indicating occasional load peaks.

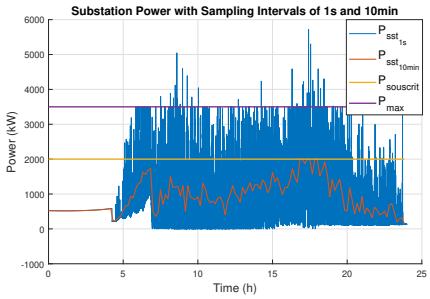

Fig. 5: Substation Power

Figure 6 illustrates the battery power along with the minimum and maximum power limitations and the pricing. The blue curve represents the battery power as given by Real-time energy management with a time step of 1 second. The red curve shows the battery power according to Day-ahead management with a time step of 10 minutes, and the green curve represents the grid pricing.

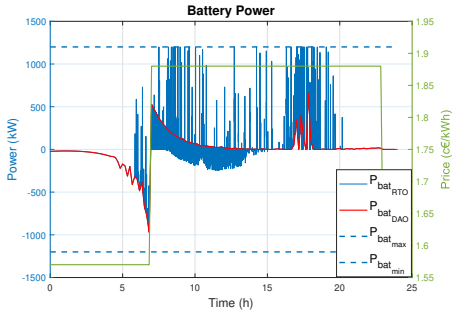

Fig. 6: Battery Power

Figure 7 shows the state of charge (SOC) of the battery. The blue curve shows the SOC with real-time energy management, while the red curve shows the SOC with day-ahead management. The two dotted lines represent the minimum and maximum SOC limits.

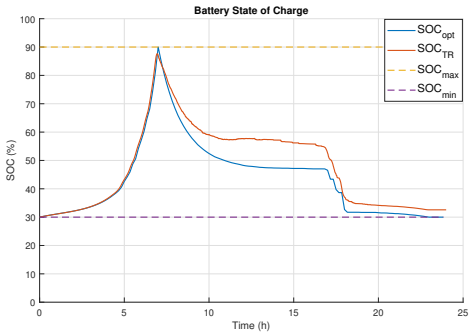

Fig. 7: State of charge

Figures 6 and 7 show that the power constraints and the battery state of charge are rigorously respected. Optimization of the battery charge is aligned with the periods when electricity tariffs are lowest, enabling energy to be stored at reduced cost. This stored energy is then used during periods when tariffs are higher, maximizing energy cost savings and reducing reliance on external energy sources during peak hours.

Real-time energy management, in line with the guidelines established by the previous day's forecasts, continually adapts the energy strategy to maintain the balance between supply and demand. This ability to adapt is important, particularly during unforeseen events such as power peaks or periods of excess renewable energy production, guaranteeing the stability of the energy system while optimizing costs.

V. Conclusions

This paper proposed an innovative method for energy management of a new smart grid railway system, as part of the RACCORD project. By integrating solar energy production systems and energy storage solutions, it aims to address the challenges posed by increasing rail traffic and the constraints of existing DC substations. The energy management system developed uses a two-stage strategy, comprising day-ahead energy management and real-time energy management. This approach optimizes energy consumption by taking advantage of periods of low electricity tariffs to store energy, which is then used during tariff peaks to minimize costs and reduce dependence on external sources.

Simulation results validate the effectiveness of this approach, showing significant adherence to power constraints and optimized battery charging strategies. The adaptability of the system to real conditions and unforeseen events, such as power peaks or overproduction of renewable energy, underlines its robustness and potential for improving the stability and efficiency of the rail energy infrastructure. Overall, the RACCORD project not only achieves a reduction in energy consumption but also paves the way for more sustainable and efficient rail networks, contributing to the wider objective of reducing the carbon footprint and improving the capacity of transport networks.

VI. Perspectives

The results obtained in this study are promising for modeling the rail smart grid and energy management. Nevertheless, in future works, a number of improvements can still be envisaged to further optimize these systems. Here are some suggested improvement strategies for future works:

1) Include the costs associated with overruns: including the penalties associated with the Monthly Overrun Pricing Component (MOPC) could help minimize overall energy costs.

$$MOPC = \sum_{i=1}^{n} \alpha \times b_i \times \sqrt{\sum_{j=1} (P_j - Ps_i)^2} \qquad (17)$$

i denotes the time range, varying from 1 to n where $n = 5$, see [15];

j : is the set of 10 minute points exceeded for time range i;

b_i : is the power weighting coefficient defined by time range i;

P_j : is the average power 10 minutes higher than the subscribed power in kW ;

Ps_i : is the subscribed power for the time range i;

α : is the weighting coefficient for the MOPC;

2) Exploit consumption forecasts: the use of consumption forecast data could refine energy management strategies and improve system efficiency.

Acknowledgment

This work received funding from the French government under the France 2030 program, specifically for the RACCORD project, and was also supported by Bpifrance.

References

[1] E. Hoda, O. Hussein, M. Stephane, G. Hamid, F. Olivier," Performance of Linear Programming in Optimizing the Energy Schedule of a Grid-connected Hybrid System Compared to Particle Swarm Optimization", NERGY 2022: The Twelfth International Conf. on Smart Grids, Green Communications and IT Energy-aware Technologies, 2022.

[2] S. Angalaeswari, K. Jamuna, "Optimal energy management using sequential quadratic programming algorithm for stand alone PV system". Intern. J. of Applied Eng. Research. 12. 12250-12255, 2017.

[3] B. Heymann, J. F. Bonnans, P. Martinon, F. J. Silva, F. Lanas, G. Jimenez-Estévez, "Continuous optimal control approaches to micro-grid energy management", Energy Systems, 1–19, 2015.

[4] J. Radosavljevic, M. Jevtic, D. Klimenta, "Energy and operation management of a microgrid using particle swarm optimization, Engineering Optimization" vol. 48, n. 5, pp. 811–830, 2016.

[5] M. Elsied, A. Oukaour, T. Youssef, H. Gualous, O. Mohammed, "An advanced real time energy management system for microgrids", Energy, Vol. 114, 2016.

[6] P. Petronela, A. Dhaker, S. Christophe, M. Othman, P. Julien, R. Benoit, "Energy Management Multi-Criteria Design for Hybrid Railway Power Substations". ELECTRIMACS 2014.

[7] C. R. Akli, X. Roboam, B. Sareni, A. Jeunesse, "Energy management and sizing of a hybrid locomotive", European Conference on Power Electronics and Applications, 2007, pp. 1-10.

[8] E. Kuznetsova, Y.-F. Li, C. Ruiz, E. Zio, G. Ault, K. Bell, "Reinforcement learning for microgrid energy management", Energy 59,pp 133–146, 2013.

[9] C. S. Karavas, G. K. Konstantinos, G. Arvanitis, G. Papadakis, "A multi-agent decentralized energy management system based on distributed intelligence for the design and control of autonomous polygeneration microgrids", Energy Conversion and Management, Vol. 103, pp 166-179, 2015.

[10] S. Gaizka, M. José, Z. Inmaculada, A. Francisco, O. Oier, "Analysis of the Current Electric Battery Models for Electric Vehicle Simulation", Energies. 12. 2750, 2019.

[11] M. Taha, '12-Pulse Active Rectifier for More Electric Aircraft Applications', Flight Physics - Models, Techniques and Technologies. InTech, Feb. 14, 2018.

[12] Bouras, Slimane and Babaammi, Nabil,Etude et réalisation d'un hacheur réversible pour une application dans un système photovoltaïque 2018

[13] Nedjma Aouchiche. Conception d'une commande MPPT optimale à base d'intelligence artificielle d'un système photovoltaïque.. Autre. Université Bourgogne Franche-Comté, 2020. Français. ffNNT : 2020UBFCA001ff. fftel-02902953

[14] Cyril Lahore. Optimisation de commandes MPPT. Automatique / Robotique. 2012. ffdumas01304277f

[15] Réseau de Transport d'Électricité (RTE), *Plaquette tarifaire TURPE 6 Consommateurs et Producteurs*, 2023. Available at : Plaquette Tarifaire Consommateurs Producteurs (services-rte.com)